Adaptor Protein-2 Exhibits $\alpha_1\beta_1$ or $\alpha_6\beta_1$ Integrin-Dependent Redistribution in Rhabdomyosarcoma Cells†

Nikhat D. Boyd,‡ Bosco M. C. Chan,§ and Nils O. Petersen*,‡

Department of Chemistry, University of Western Ontario, London, Ontario N6A 5B7, Canada, and Department of Microbiology and Immunology and Robart's Research Institute, University of Western Ontario, 100 Perth Drive, London, Ontario N6A 5K8, Canada

Received July 19, 2001; Revised Manuscript Received February 21, 2002

ABSTRACT: Downregulation of several signaling pathways, such as those stimulated by growth factor receptors, occurs by internalization of signaling receptors through clathrin-coated pits. The first step in internalization or endocytosis is interaction with AP-2, which results in coated pit formation by assembly of clathrin to AP-2. Changes in endocytosis are reflected in the distribution of AP-2 molecules at the cell surface. Integrins are receptors which mediate attachment to the extracellular matrix and also stimulate numerous intracellular signaling pathways; however, it is not known how signaling through integrins is terminated or downregulated. Endocytosis through clathrin-coated pits offers an attractive mechanism for this. This work explores the relationship between AP-2 and β_1 integrins. RD cells grown for 24 h on collagen or laminin exhibit a redistribution of AP-2 to the cell periphery relative to those grown on fibronectin or polylysine. The total AP-2 protein levels in the cells are unaffected. Blocking $\alpha_1\beta_1$ integrin ligand binding on collagen prevents this redistribution fully. On laminin where $\alpha_1\beta_1$ and $\alpha_6\beta_1$ integrins are engaged, both receptors must be simultaneously blocked to prevent AP-2 redistribution, confirming that the redistribution depends on the specific engagement of the receptors. Immunofluorescence reveals that the majority of $\alpha_1\beta_1$ integrins colocalize with $\alpha_6\beta_1$ integrins in linear structures identified as focal adhesions. A separate fraction of $\alpha_1\beta_1$ integrins colocalize with AP-2 in coated pits. Interestingly, $\alpha_6\beta_1$ integrins are not located in coated pits, demonstrating that integrin colocalization with AP-2 is not necessary to induce redistribution of AP-2.

AP-2[1] is a tetrameric protein consisting of two 100 kDa adaptin subunits (α and β2), a medium subunit (μ2), and a small subunit (σ2) (*1*). Rapid freeze, deep etch images of AP-2 demonstrate that it is comprised of a brick-shaped core or trunk region with two appendage domains that extend from either side, corresponding to the C-termini of the adaptin subunits (*2*). AP-2 recognizes specific amino acid sequences on receptors targeted for endocytosis (*3*, *4*), which initiates formation of clathrin-coated pits (*5*). Clathrin has three legs radiating from a central hub, and this structure is called a triskelion (*6*). Assembly of the triskelions into pentagon and hexagon shapes forms the characteristic lattice structure of the coated pit (*7*). AP-2 interacts with clathrin via a portion of its β2 subunit located in the trunk region of the molecule (*8*−*10*). A coated pit typically consists of approximately 120 clathrin triskelions (*11*). It is estimated that a single AP-2 tetramer interacts with two clathrin triskelions so that there are 60 AP-2 molecules per coated pit (*2*, *8*, *12*). The majority of AP-2 is localized to the plasma membrane (*13*), and in addition to its interaction with clathrin, AP-2 is also known to interact with a number of other proteins involved in the endocytic process. AP-2 associates via its appendage domain with the EGF receptor kinase substrate, Eps15, in a constitutive manner (*14*). Microscopy studies revealed that Eps15 is located at the rim of budding coated vesicles (*15*). This protein may play a role in endocytosis as Eps15 mutants that interfere with coated pit assembly inhibit transferrin receptor endocytosis (*16*). Eps15 and AP-2 are both able to interact with epsin, which is also thought to be important in endocytosis when acting in concert with Eps15 (*17*). The appendage domain of AP-2 has also been implicated in interaction with dynamin, a protein required for the fission of coated vesicles from the membrane (*18*) and with amphiphysin in synaptic nerve terminals (*19*), which is believed to be involved in the recruitment of dynamin (*20*).

Previous work reveals that AP-2 exists in two distinct populations in CV-1 cells (*21*). Two-thirds of all AP-2 molecules are found in larger aggregates of approximately 60 AP-2 proteins associated with coated pits, and the remaining AP-2 population is distributed in smaller aggregates of, on average, 20 AP-2 molecules which are proposed to be nucleation sites for coated pit formation. An increase in endocytosis activity is reflected in a redistribution

† This work was supported in part by operating grants from the Natural Sciences and Engineering Research Council (NSERC), Ottawa, Canada, and the Canadian Institute of Health Research (CIHR) and by a CIHR Studentship award.

* To whom correspondence should be sent: (519) 661-2111 ext 86333 (phone); (519) 661-3022 (fax); petersen@julian.uwo.ca (e-mail).

‡ Department of Biochemistry, University of Western Ontario.

§ Department of Microbiology and Immunology and Robart's Research Institute, University of Western Ontario.

[1] Abbreviations: ECM, extracellular matrix; AP-2, adaptor protein-2; RD, rhabdomyosarcoma; ICS, image correlation spectroscopy; CD, cluster density; DA, degee of aggregation; TGN, trans-Golgi network; PBS, phosphate-buffered saline; BSA, bovine serum albumin; mAb, monoclonal antibody; pAb, polyclonal antibody; EGF, epidermal growth factor; LDL, low-density lipoprotein.

10.1021/bi011501f CCC: $22.00
Published on Web 05/11/2002

of AP-2 molecules from smaller AP-2 clusters comprising nucleation sites into already existing coated pits (*22*, *23*).

It is well established that a number of signaling receptors are downregulated through internalization via clathrin-coated pits (*24*−*27*). Integrins act as receptors for extracellular matrix (ECM) proteins, participate in organizing cell adhesion complexes, and mediate signal transduction (*28*−*30*). The mechanism of their downregulation is not clearly defined. They are a family of cell surface receptors composed of α and β heterodimers. The interaction with the ECM through integrins is crucial for cell proliferation, differentiation, and migration (*31*, *32*). Integrin binding to ECM proteins results in the formation of adhesion complexes termed focal adhesions or focal complexes (*33*). This process leads to reorganization of cytoskeletal components, including actin, which serve as scaffolding proteins for intracellular effector molecules to couple integrins to downstream signaling events (*31*).

Receptors targeted for endocytosis bind to AP-2, which recruits clathrin to form a coated pit that subsequently invaginates and forms a coated vesicle (*26*, *34*). It is possible that endocytosis downregulates integrin receptors, but the evidence is indirect. Microscopy studies indicate that a large proportion of integrins are located in intracellular compartments (*35*, *36*). Mutations of the integrin β_1 cytoplasmic domain, which cause increased levels of bacterial internalization, also inhibit the localization of these receptors to focal adhesions (*37*). Other experiments show that both focal adhesions and clathrin-coated membrane regions are sites of cell substratum adhesion; as clathrin-coated membranes do not have intrinsic adhesive properties, adhesion would have to occur by another mechanism, indicating a possible role for integrins (*38*).

AP-2 has been shown to recognize specific sequences in the cytosolic tails of transmembrane receptors to direct their internalization (*39*). Although it has been suggested that the β2 adaptin subunit may be involved in recognition of receptor tails (*40*, *41*), the most compelling evidence suggests that the μ2 subunit is responsible for receptor binding at the plasma membrane (*42*). Internalization signals are characterized by an essential tyrosine residue of a YXXø motif, where ø represents a bulky hydrophobic amino acid (*43*) or an NPXY motif (*44*, *45*). There is also a dileucine motif which is recognized by the β1 subunit in AP-1, the adaptor protein involved in coated pit formation at the TGN (*46*). The β_1 integrin cytosolic tail contains two NPXY sequences allowing for potential recognition by AP-2 and downregulation of these receptors through coated pits.

The β_1 family of integrins has major functions in mediating cell adhesion to ECM proteins such as fibronectin, collagen, and laminin (*47*). A single receptor is often able to bind more than one extracellular matrix protein, and similarly a single extracellular matrix protein often engages multiple integrins (*48*). In rhabdomyosarcoma (RD) cells, $\alpha_4\beta_1$ and $\alpha_5\beta_1$ integrins bind fibronectin, $\alpha_1\beta_1$ integrins binds collagen, and both $\alpha_1\beta_1$ and $\alpha_6\beta_1$ integrins bind laminin (*49*).

In the present work, we have explored whether endocytosis through clathrin-coated pits is a mechanism for downregulation of integrin-mediated signaling. Quantitative analysis of confocal fluorescence images is used to determine changes in distribution and localization of AP-2 in response to adhesion and growth on specific extracellular matrix proteins. The specificity of the responses are determined with antibodies known to block selected integrin−substrate interactions. Finally, the interactions between the integrins and the AP-2 are probed by measurements of the extent of colocalization in confocal images of doubly immunolabeled cells.

MATERIALS AND METHODS

Cell Culture. Rhabdomyosarcoma RD cells from the American Type Culture Collection (Rockville, MD) were maintained in RPMI 1640 medium supplemented with 10% FBS, glutamine, and penicillin/streptomycin at 37 °C (complete RPMI), 100% humidity, and 5% CO_2. Cells were passaged approximately every 3 days to maintain exponential growth.

Antibodies. For immunolabeling of AP-2, both the monoclonal antibody (mAb) AC1-M11 and a polyclonal antibody (pAb) were used. AC1-M11 was a gift from Margaret S. Robinson (University of Cambridge, U.K.), and the pAb was a gift from Thomas Kirchhausen (Harvard University, Boston, MA). This polyclonal antibody is used at saturating conditions as determined by titration measurements in these cells. They are specific for AP-2 since they block binding of specific monoclonal antibodies (AP-6) and can be blocked by AP-6. Immunostaining of the $\alpha_1\beta_1$ or $\alpha_6\beta_1$ integrins was achieved using the α_1-specific mAb TS2/7 or the α_6-specific mAb MA6 conjugated to AlexaFluor 594 using the AlexaFluor 594 protein labeling kit according to manufacturer's instructions (Molecular Probes, Inc., Eugene, OR). In cases where both the $\alpha_1\beta_1$ and $\alpha_6\beta_1$ integrins were visualized, unconjugated versions of either the MA6 or TS2/7 antibodies were used in conjunction with fluorescein-conjugated goat anti-mouse antibodies. Integrins were blocked using the α_1-specific mAb FB12 and the α_6-specific mAb GoH3. Vinculin visualization was achieved with the mAb V284 (Chemicon International, Inc., Temecula, CA).

Cell Adhesion to ECM Substrates. Twenty-two millimeter coverslips were washed in 95% ethanol and allowed to dry. Five hundred microliters of human fibronectin, collagen I, laminin 1, or polylysine (Gibco BRL, Rockville, MD) was applied to cover the surface of the coverslips. Protein concentrations were 10 μg/mL in 0.1 M $NaHCO_3$ except where otherwise indicated. Coverslips were enclosed in 35 mm culture dishes and placed in a container lined with damp paper towel at 4 °C for a period of 14−18 h. Coverslips were rinsed with 1.5 mL each of PBS, doubly distilled water, and complete RPMI medium and placed in 35 mm culture dishes. RD cells were added at a density of 1.5×10^5 cells per 35 mm dish in complete RPMI medium. Cells were incubated at 37 °C for a period of 24 h prior to fixation. In experiments using integrin blocking antibodies, cells were incubated with 100 μL of complete RPMI containing 10 μg/mL blocking antibody for 1 h on ice prior to addition onto coverslips. Antibodies used for blocking were FB12 for $\alpha_1\beta_1$ integrins or GoH3 for $\alpha_6\beta_1$ integrins.

Fixing and Immunostaining Cells. Cells were rinsed three times in cold PBS prior to being fixed. When labeling with the AP-2-specific pAb, cells were fixed with 4.4% paraformaldehyde in PBS for 10−15 min and then permeabilized with 0.04% saponin in PBS for 10 min on ice. In all other cases cells were fixed for 5 min in methanol at −20 °C followed by 2 min in acetone at −20 °C.

Prior to immunostaining, cells were washed twice with PBS and one time with PBS containing 2% BSA. For AP-2 localization, cells were incubated first with 20 μL of 200 μg/mL normal goat IgG for 40−60 min and then with 20 μL of 50 μg/mL AC1-M11 or 20 μL of AP-2 pAb (1:100 dilution) for 90−120 min. Finally, cells were incubated with 20 μL of 20 μg/mL fluorescein-conjugated goat anti-mouse antibody in the case of the mAb or with 20 μL of 50 μg/mL fluorescein-conjugated goat anti-rabbit antibody in the case of the pAb for 60−90 min. In experiments where both AP-2 and $\alpha_1\beta_1$ or $\alpha_6\beta_1$ integrins were to be localized, AP-2 was labeled first with mAb AC1-M11 (as indicated above) followed by incubation with 20 μL of 200 μg/mL normal mouse IgG for 40−60 min and then by incubation with 20 μL of 25 μg/mL AlexaFluor 594 conjugated α_1-specific mAb TS2/7 or α_6-specific mAb MA6 for 90−120 min. In experiments where both $\alpha_1\beta_1$ and $\alpha_6\beta_1$ integrins or $\alpha_1\beta_1$ integrins and vinculin were to be localized, either $\alpha_6\beta_1$-integrins or vinculin was labeled first by incubations with 20 μL of 200 μg/mL normal goat IgG for 40−60 min and then 20 μL of 50 μg/mL MA6 for $\alpha_6\beta_1$ integrins or V284 (1:25) for vinculin for 90−120 min, followed by 20 μL of 20 μg/mL fluorescein-conjugated goat anti-mouse antibody for 60−90 min. The $\alpha_1\beta_1$ integrin was visualized using the AlexaFluor 594 conjugated TS2/7 mAb as described above. Between antibody incubations, cells were washed three times with PBS and once with PBS containing 2% BSA for 5−10 min each time while being agitated on a tilt table (Wave-Master, Vantronics, London, Ontario). Finally, coverslips were mounted on slides using Airvol containing *n*-propyl-gallate and stored at 4 °C in the dark. In all cases, saturating antibody concentrations were employed as determined using ICS measurements (*50*).

Image Collection (Confocal Microscopy) and Analysis. Images were collected with a Bio-Rad MRC-600 confocal microscope equipped with an argon/krypton mixed gas laser on an inverted Nikon microscope. The total laser power is nominally 25 mW, and images were collected at 1% laser power by attenuation with a neutral density filter. Fluorescein was visualized by excitation at 488 nm while AlexaFluor 594 was visualized by excitation at 568 nm. In cases where both chromophores were used, fluorescein emission was first collected from photomultiplier tube 2 and then AlexaFluor 594 emission was collected from photomultiplier tube 1.

To obtain images for ICS analysis, individual fluorescent cells were localized using a 60× objective and mercury lamp illumination. An image of 15.5 μm × 15.5 μm from an area selected from the periphery of the cell was collected with the laser using a zoom factor of 10 in photon counting mode to ensure linear amplification of the intensity signal. Between 15 and 25 scans were accumulated to produce a single image. Only one image was collected per cell. In regions where images were obtained, cells were sufficiently thin so that there was only a single focal plane. For each data point, between 35 and 40 images from individual cells were analyzed. Black levels were maintained at 5.9 on the vernier scale, and the gain was set at 10.0.

To obtain images for whole cell analysis, confocal images of an entire cell were taken at 2 μm intervals along the *z*-direction. The set of seven images from a distance of 12 μm was projected to form a single image. The cell perimeter was then outlined, and the intensity within the total cell interior was determined. This was repeated for 30−40 cells per experiment, and an average value from two to three experiments was determined.

Image correlation spectroscopy analysis was performed on a MasPar 2 with 2048 parallel processors (MP-2, MasPar Corp., Sunnyvale, CA). Correlation calculations were performed as described earlier (*21*, *51*, *52*), and the correlation functions $g(\xi,\eta)$ were fit to a two-dimensional Gaussian function according to the equation:

$$g(\xi,\eta) = g(0,0)e^{-(\xi^2+\eta^2)/\omega^2} + g_0 \quad (1)$$

Here ξ and η are the position lag coordinates for the *x* and *y* axes, respectively, and ω is the radius of the laser beam. The amplitude of the correlation function as ξ and η approach zero is given by $g(0,0)$. The offset, g_0, is included to account for incomplete decay at larger distances arising from limited image size.

A cluster density (CD) value, which represents the average number of independent protein particles (Np) per unit area, is defined according to the equation:

$$\mathrm{CD} = \frac{1}{g(0,0)\pi\omega^2} = \frac{\bar{\mathrm{N}}\mathrm{p}}{\pi\omega^2} \quad (2)$$

A third parameter, the degree of aggregation (DA), represents the average number of molecules in the protein aggregates and is obtained by dividing the average total number of protein monomers (Nm), which is estimated by the average fluorescence intensity ($\langle i(x,y)\rangle$), by the average number of independent protein particles (Np) according to the equation:

$$\mathrm{DA} = \langle i(x,y)\rangle g(0,0) = \alpha\frac{\bar{\mathrm{N}}\mathrm{m}}{\bar{\mathrm{N}}\mathrm{p}} \quad (3)$$

where α is a constant involving instrumental and experimental parameters.

Statistical Analysis. Typically, between 35 and 40 images were collected for a single experiment. Pooled data from a minimum of three experiments were compared using Student's *t*-test. Significance was assigned to those results that yielded *p* values less than 0.001.

RESULTS

Confocal images of an RD cell immunostained to visualize AP-2 are shown in Figure 1. Figure 1A shows a view of the entire cell. Figure 1B is an example of an image used for correlational analysis and corresponds to the boxed region in Figure 1A. It is collected with a 10-fold increased magnification compared to Figure 1A and is taken from an area near the cell periphery where the cell is thin and there is minimal contribution from cytosolic fluorescence. The punctate staining pattern is characteristic of AP-2 and represents the coated pit population (*53*).

Figure 2 demonstrates that the total cellular fluorescence intensity (black bars) contributed by AP-2 was similar when RD cells adhered for 24 h to fibronectin, collagen, or laminin and did not differ significantly from control cells grown on polylysine. This establishes that there is no effect on total AP-2 levels induced by different extracellular matrices in a 24 h period.

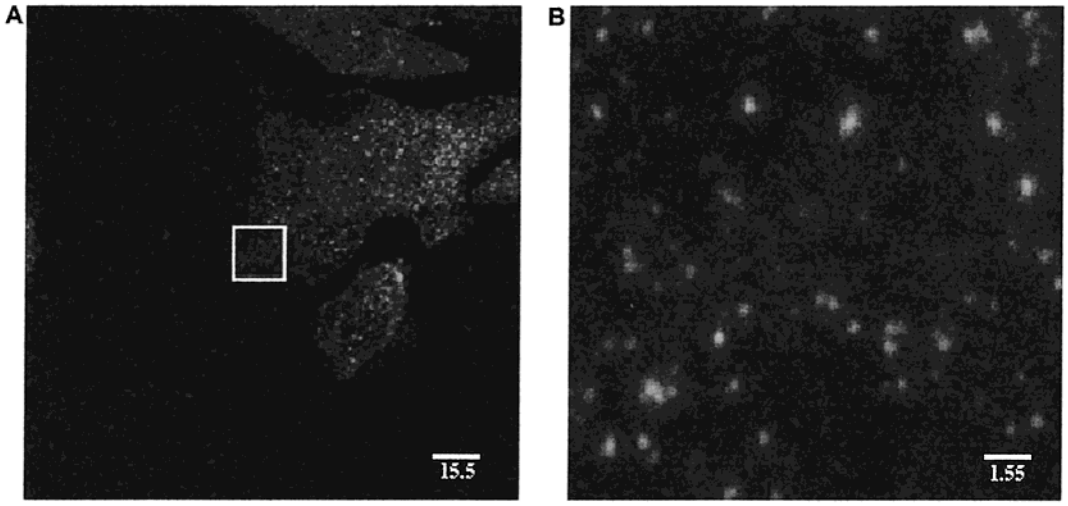

FIGURE 1: RD cells grown on laminin for 24 h and stained with AP-2 antibody, AC1-M11. Scale bars are shown in micrometers. An image of a cell taken at lower magnification showing AP-2 staining in the entire cell (A, scale bar represents 15.5 μm). An image of the indicated box in (A) enlarged 10 times (B, scale bar represents 1.55 μm). This is a sample of an image that is used for ICS analysis. Scale bars are shown in micrometers.

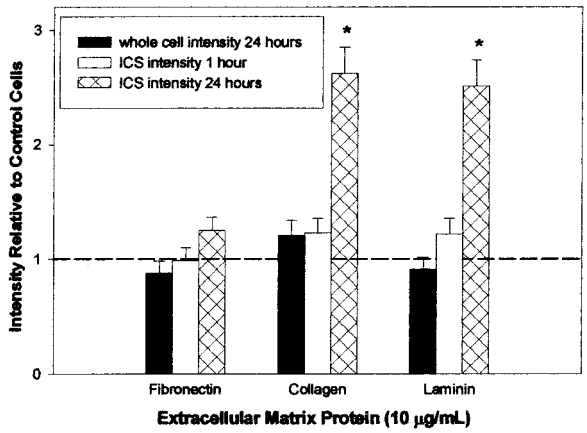

FIGURE 2: RD cells grown for 1 or 24 h on 22 mm coverslips coated with either 10 μg/mL polylysine or 10 μg/mL indicated extracellular matrix proteins were fixed and immunofluorescently labeled for AP-2 as described in Materials and Methods. Data were normalized to control cells grown on polylysine [$N = 32$ (whole cell intensity), $N = 99$ (1 h), $N = 80$ (24 h)]. Error bars indicate SEM. Whole cell fluorescence intensity of AP-2 in RD cells grown on the indicated substrates (black bars) ($N = 32$ for each). ICS analysis of fluorescence intensity in the cell periphery after 1 h (white bars) [$N = 99$ (fibronectin), $N = 101$ (collagen), $N = 94$ (laminin)] or 24 h (hatched bars) [$N = 81$ (fibronectin), $N = 76$ (collagen), $N = 82$ (laminin)]. Asterisks (*) indicate $p < 0.001$ compared to polylysine controls.

AP-2 fluorescence intensity measured from the cell periphery (Figure 1B) after 1 h on either fibronectin, collagen, or laminin was comparable to that of control cells grown on polylysine (Figure 2, white bars). However, after 24 h there was a greater than 2-fold increase in the AP-2 fluorescence intensity in the area of the cell periphery in cells grown on either collagen or laminin compared to cells grown on polylysine or fibronectin (Figure 2, hatched bars). AP-2 fluorescence intensity in cells grown on fibronectin for 24 h was not significantly different from cells grown on polylysine. If cells are grown on a polylysine matrix in the absence of serum, they maintain a rounded morphology and do not spread within the 24 h time period. Cells under these experimental conditions cannot be used for ICS since images collected for correlational analysis must be taken from the cell periphery where cells are both thin and flat so there is minimal cytosolic contribution and the entire image can be in focus. This problem is circumvented by using control cells grown on polylysine in the presence of serum so they are able to spread. The distribution of AP-2 was compared on fibronectin, collagen, and laminin in both the presence or absence of serum. In all three cases, the AP-2 distribution was unaffected by the addition of serum (data not shown). These experiments therefore can probe the differential effects of collagen, laminin, or fibronectin. The intensity data in Figure 2 indicate that the collagen and laminin matrices induce a redistribution of AP-2 proteins away from the middle of the cell into the cell periphery between 1 and 24 h of growth rather than inducing a general increase in the total amount of AP-2 in the cell.

Figure 3 shows that laminin concentrations of 1 μg/mL are sufficient to induce movement of the AP-2 protein population into the cell periphery compared to control cells grown on polylysine. It appears that a minimum concentration of laminin is required to trigger a nearly complete redistribution of AP-2 as cells grown on 0.1 μg/mL laminin did not differ significantly from control cells. A concentration of 10 μg/mL laminin is sufficient to induce a maximal redistribution of AP-2 since increasing the laminin concentration to 50 μg/mL does not have additional effects on the response; thus, laminin at 10 μg/mL was used for the subsequent experiments. Comparison of the AP-2 intensity values obtained for either 1, 10, or 50 μg/mL laminin reveals that they are statistically equivalent. The intensity value obtained here for 10 μg/mL laminin was statistically equivalent to the intensity value obtained on laminin in Figure 2.

To establish whether the observed redistribution is integrin specific, the AP-2 distributions on collagen and laminin were examined in the presence of antibodies that prevent integrin binding to these ECM proteins. The AP-2 distribution in cells grown on polylysine was unaffected by incubation with either a control nonspecific antibody, an $\alpha_1\beta_1$ functional blocking antibody (FB12), or an $\alpha_6\beta_1$ functional blocking antibody (GoH3) (data not shown). Figure 4A shows that the

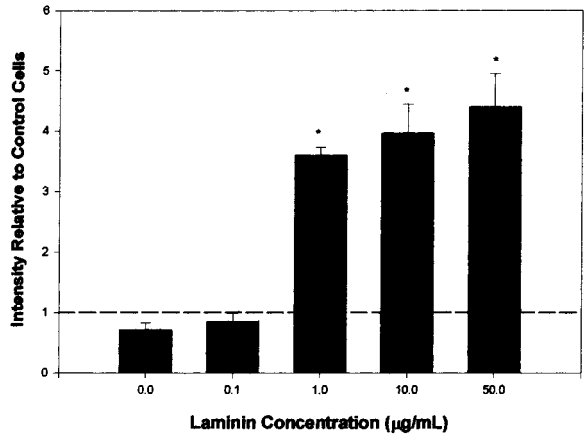

FIGURE 3: RD cells grown on 22 mm coverslips coated with various concentrations of laminin ($N = 63$, 62, 62, 62, and 63 for increasing laminin concentrations, respectively, beginning with 0 μg/mL) for a period of 24 h were fixed and immunolabeled for AP-2 as described in Materials and Methods. ICS analysis yielded intensity values which were normalized to data obtained in control cells grown on polylysine ($N = 65$). Error bars indicate SEM. Asterisks (*) indicate $p < 0.001$ compared to polylysine controls. Comparison of either the relative intensity or absolute intensity values obtained on 10 μg/mL laminin in Figure 2 and this figure were not significantly different ($p = 0.0816$ for absolute values; $p = 0.389$ for relative values).

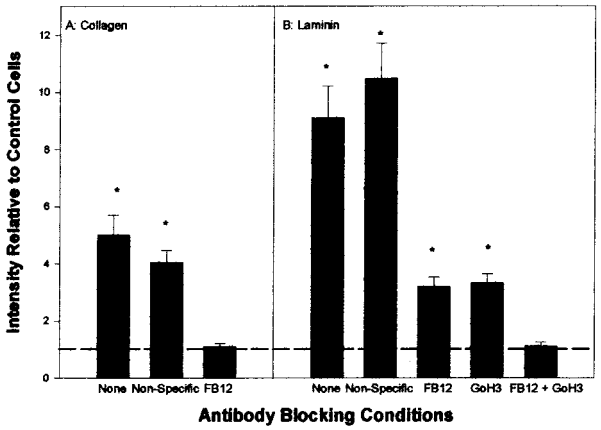

FIGURE 4: RD cells were incubated on ice for 1 h in the absence of antibody [$N = 65$ (A), $N = 92$ (B)] or with either 10 μg/mL nonspecific control antibody [$N = 61$ (A), $N = 109$ (B)], FB12 mAb [$N = 63$ (A), $N = 110$ (B)], GoH3 mAb ($N = 91$), or both FB12 and GoH3 mAbs ($N = 98$). These antibodies functionally block the integrin receptors. Cells were then plated onto coverslips coated with either 10 μg/mL collagen (A) or 10 μg/mL laminin (B) and grown for 24 h before being fixed and immunostained for AP-2 as described in Materials and Methods. ICS analysis yielded intensity values which were normalized to control cells incubated with the FB12 mAb prior to plating on polylysine. Error bars indicate SEM. Asterisks (*) indicate $p < 0.001$ compared to controls.

redistribution of AP-2 to the outer regions of cells grown on collagen is completely inhibited by incubation with FB12. In contrast, Figure 4B shows that the redistribution of AP-2 on laminin was reduced when cells were incubated with either the FB12 or GoH3 antibodies. However, when both of these antibodies were used in combination, the level of AP-2 redistribution was reduced to the level of that observed in RD cells grown on polylysine. This indicates that binding of both $\alpha_1\beta_1$ and $\alpha_6\beta_1$ integrins to laminin contributes to the observed redistribution of AP-2. There is no significant difference between the intensity values observed when cells are incubated with either FB12 or GoH3 alone, indicating that the $\alpha_1\beta_1$ and $\alpha_6\beta_1$ integrins affect AP-2 redistribution to the same extent.

The relative increases in fluorescent intensity in Figure 4 are higher than those observed in Figure 2. This is partially because two different AP-2 antibodies were used to collect these data; a mAb was used for Figure 2 and a pAb was used for Figure 4. The integrin blocking experiments shown in Figure 4 required the use of a pAb directed against AP-2 in order to prevent the cross-reactivity of the fluorescently labeled secondary antibody with the monoclonal integrin blocking antibodies. Attempts to directly conjugate the AP-2 mAb to a fluorescent label were unsuccessful. The pAb results in a more diffuse staining pattern, possibly due to the stoichiometry of its binding to AP-2 molecules, and this might contribute to differences in results obtained using this antibody compared to the AP-2 mAb.

The observed increase of AP-2 in the periphery of cells grown on collagen or laminin could occur in either of two ways. The AP-2 from the center portion of the cell (away from the cell edges) may be recruited to existing peripheral AP-2 aggregates of AP-2 proteins, resulting in the formation of larger coated pits which would be observed as an increase in the degree of aggregation (DA). Alternatively, the AP-2 proteins may be recruited to regions of the cell periphery which are unoccupied by other AP-2 molecules, to form new aggregates or coated pits, resulting in an overall increase in the density of AP-2 clusters which would be observed as an increase in cluster density (CD). To distinguish between these two possibilities, AP-2 distributions in RD cells grown on different ECM proteins were analyzed using image correlation spectroscopy. The parameters calculated are the average aggregate size as measured by DA (eq 3) and the density of clusters as measured by CD (eq 2). Corresponding intensity data are shown in Figure 2. As expected, the aggregate size (black bars) and the density of AP-2 clusters (white bars) on fibronectin were the same as those in cells grown on polylysine (Figure 5). Results obtained on collagen reveal that the average size of the AP-2 aggregates in the cell periphery is approximately 2-fold greater than the average aggregate size observed in cells grown on polylysine while the cluster density remains unaffected; on laminin, both the aggregate size and the cluster density increase compared to cells grown on polylysine (Figure 5).

Since the recruitment of AP-2 to the periphery is dependent on the specific engagement of $\alpha_1\beta_1$ and $\alpha_6\beta_1$ integrins, it is possible that AP-2 is needed to downregulate these integrins. This implies direct association of integrins with coated pits which should be observed as a colocalization of integrins and AP-2. To determine whether this occurs, RD cells grown on laminin for 24 h were labeled with mAbs to either $\alpha_1\beta_1$ (Figure 6A) or $\alpha_6\beta_1$ integrins (Figure 6C) and AP-2 (Figure 6B,D) using different chromophores. Figure 6 shows representative examples of images from at least four separate experiments in each of which a minimum of 10 cells was examined. We observed that both $\alpha_1\beta_1$ and $\alpha_6\beta_1$ integrins were organized in filamentous structures radiating away from the nucleus toward the edges of the cell whereas the AP-2 was distributed into a punctate pattern characteristic of coated pits (*21*, *22*). High magnification images of AP-2 and either $\alpha_1\beta_1$ (Figure 6E) or $\alpha_6\beta_1$ (Figure 6F) were overlaid to

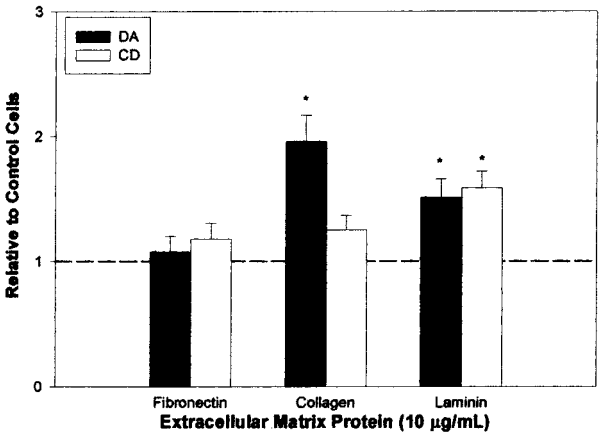

FIGURE 5: RD cells grown on 22 mm coverslips coated with 10 μg/mL polylysine, fibronectin, collagen, or laminin for 24 h were fixed and immunolabeled for AP-2 with the monoclonal AP-2 antibody, AC1-M11, as described in Materials and Methods. Aggregate sizes (DA, black bars) and cluster densities (CD, white bars) were calculated from data obtained by ICS analysis [$N = 81$ (fibronectin), $N = 76$ (collagen), $N = 82$ (laminin)] and normalized to data obtained in control cells grown on polylysine ($N = 80$). The corresponding intensity data are shown in Figure 2. Error bars indicate SEM. Asterisks (*) indicate $p < 0.001$ compared to controls.

determine whether there was colocalization. Almost all of the AP-2 colocalized with $\alpha_1\beta_1$ integrins in coated pit structures (Figure 6E, arrows); however, the linear structures where the majority of $\alpha_1\beta_1$ integrins were distributed did not contain any AP-2. Shifting the AP-2 image 0.4 μm to the left (Figure 6G) resolves the individual red and green chromophores in the coated pits, confirming the colocalization between AP-2 and $\alpha_1\beta_1$. Thus, it seems that $\alpha_1\beta_1$ integrins are organized into two populations: the majority of $\alpha_1\beta_1$ is found in linear or filamentous structures and a smaller fraction colocalizes with AP-2 in coated pits. To resolve whether a similar colocalization occurred between AP-2 and $\alpha_6\beta_1$ integrins, the corresponding overlays of high magnification images were analyzed (Figure 6F). Surprisingly, AP-2 did not colocalize with $\alpha_6\beta_1$ integrins in coated pits (Figure 6F, arrows). However, like $\alpha_1\beta_1$ integrins, $\alpha_6\beta_1$ integrins are also organized in filamentous structures. Shifting the AP-2 image 0.4 μm to the left did not reveal any $\alpha_6\beta_1$ integrin in coated pits that may have been undetected in the direct overlay (Figure 6H).

To confirm that the linear structures correspond to integrins in focal adhesion complexes, the distribution of $\alpha_1\beta_1$ integrins and vinculin was examined. Confocal images of a cell labeled for $\alpha_1\beta_1$ (Figure 7A) and vinculin (Figure 7B) reveal similar filamentous patterns. Overlays at higher magnification reveal that these two proteins colocalize in the same linear structures, confirming them to be focal adhesions (Figure 7E). This observation is illustrated by shifting the vinculin image 1.8 μm to the left (Figure 7G). It is also apparent that there are some punctate areas where $\alpha_1\beta_1$ integrins do not colocalize with vinculin (Figure 7E,G, arrows). The pattern of this fraction of $\alpha_1\beta_1$ does not appear filamentous and might represent coated pits.

To determine whether both $\alpha_1\beta_1$ and $\alpha_6\beta_1$ integrins colocalize in the same focal adhesions, cells were doubly labeled with mAbs against each of these receptors. Individual images of cells labeled with $\alpha_1\beta_1$ (Figure 7C) and $\alpha_6\beta_1$ (Figure 7D) integrins reveal characteristic focal adhesions. A higher magnification overlay image (Figure 7F) illustrates strong colocalization between these two integrins in linear focal adhesion structures. It is also clear that there are areas where $\alpha_1\beta_1$ integrins do not colocalize with $\alpha_6\beta_1$ integrins (Figure 7F, arrows). This further confirms that $\alpha_1\beta_1$ integrins are localized in both coated pits and focal adhesions while $\alpha_6\beta_1$ integrins are found only in focal adhesions. Resolving the green and red chromophores by shifting the $\alpha_6\beta_1$ integrin image 1.8 μm slightly to the left confirms the strong colocalization of the two receptors in focal adhesions. The images in Figure 7 are representative examples of analyses of a minimum of 10 cells from each of two separate experiments.

DISCUSSION

Fluorescent images can provide compelling but qualitative information about protein distribution and localization in individual cells. Image analysis provides a means to quantify the information in individual images and to average the observations from hundreds of images to get representative population statistics. Image correlation spectroscopy (ICS) analysis performed at saturating conditions provides simultaneous information about the average number of receptors, the number of clusters they assemble into, and the average number of receptors in each cluster (*54*). This has been demonstrated for the aggregation of influenza hemagglutinin proteins containing specific mutations targeting them to coated pits (*23*). ICS allows for detection of changes in receptor distribution that might otherwise not be detected by conventional microscopic techniques. The greatest source of variability in ICS measurements occurs between cells, which has a relative error of between 35% and 45% associated with it. The relative error due to instrumental uncertainty is approximately 4.5% (*55*).

The distribution of AP-2 proteins at the cell surface in cells grown for a period of 24 h on collagen and laminin differs significantly from that on fibronectin or polylysine. This difference in distribution is mediated specifically by $\alpha_1\beta_1$ integrins on collagen and by both $\alpha_1\beta_1$ and $\alpha_6\beta_1$ integrins on laminin. This was demonstrated by blocking ECM binding of these integrins with antibodies which prevented the redistribution of AP-2. Though $\alpha_1\beta_1$ integrins are found in association with both AP-2 and focal adhesions, the inhibition of integrins is likely occurring in adhesion structures as opposed to coated pits. This is supported by the observation that blocking the engagement of $\alpha_6\beta_1$ integrins, which are found exclusively in focal adhesions, also attenuates AP-2 redistribution to the cell periphery. On collagen, the redistribution of AP-2 manifests itself as larger AP-2-containing aggregates. On laminin, the AP-2 redistribution results in an increase in both the number and size of aggregates. While this observed redistribution of AP-2 is intriguing, it is not yet clear what its significance is. It may be that $\alpha_1\beta_1$ integrins function to increase AP-2 aggregate size while $\alpha_6\beta_1$ integrins increase AP-2 cluster density. In CV-1 cells, increased endocytosis activity coincided with an increase in the average size of AP-2-containing aggregates as the adaptors moved from their nucleation sites into existing coated pits (*21*, *22*).

It is probable that a movement of AP-2 to the periphery of the cell would be coincident with an increase in endocy-

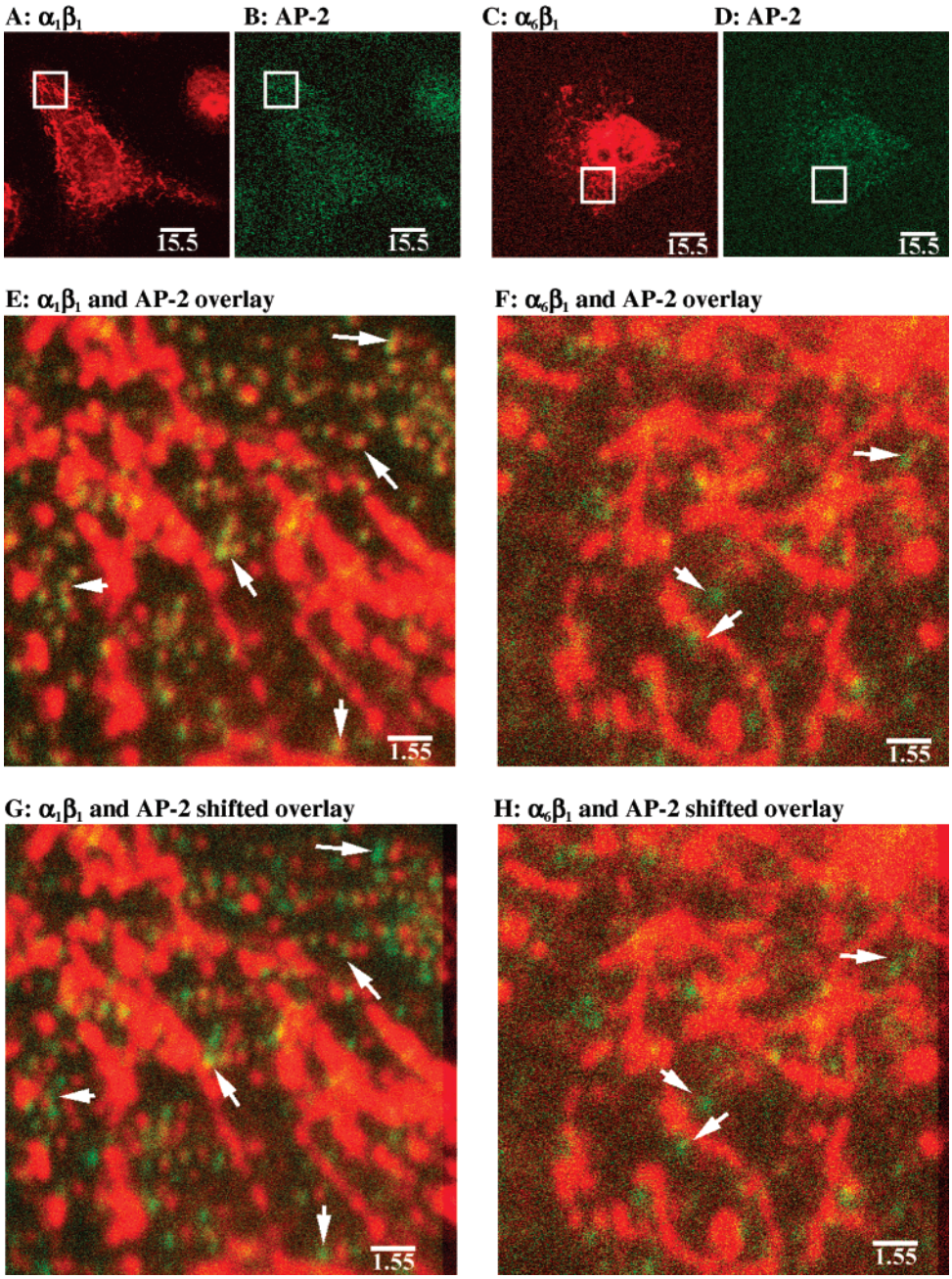

FIGURE 6: Confocal images of RD cells grown on laminin for 24 h. Scale bars are shown in micrometers. AP-2 immunolabeling is shown in green (B, D). Either $\alpha_1\beta_1$ (A) or $\alpha_6\beta_1$ (C) integrins are shown in red. Low magnification images (scale bar represents 15.5 μm) show the same cell labeled for $\alpha_1\beta_1$ (A) and AP-2 (B) or $\alpha_6\beta_1$ (C) and AP-2 (D). The boxed areas in these images were reimaged at a 10-fold greater magnification (scale bar represents 1.55 μm), and green and red images were overlaid to demonstrate colocalization. The higher magnification images from cells shown in (A) and (B) immunolabeled for $\alpha_1\beta_1$ and AP-2, respectively, are shown in (E), and the higher magnification images from cells shown in (C) and (D) immunolabeled for $\alpha_6\beta_1$ and AP-2, respectively, are shown in (F). Regions where the green and red overlap will result in yellow. Coated pits are indicated by the arrows. The green (AP-2) images from these overlays (E, F) were shifted 0.4 μm to the left to better visualize individual chromophores.

tosis in that region. Indirect association between coated pits and integrins has been previously shown using fluorescence microscopy, which demonstrated the presence of integrins in intracellular compartments thought to be endocytic vesicles (*36*). Clathrin has also been detected in adhesion sites (*38*). The present work shows that stimulation of $\alpha_1\beta_1$ and $\alpha_6\beta_1$ integrins is responsible for AP-2 redistribution and possibly an increase in endocytic activity. Such enhanced internalization would provide a mechanism for the downregulation of integrin-mediated signaling. It is clear from Figure 6 that most of the AP-2 population in coated pits contains $\alpha_1\beta_1$ integrins. Though we do not have direct evidence that $\alpha_1\beta_1$ integrins are being internalized, AP-2 is known to target receptors for internalization (*56*, *57*). However, $\alpha_1\beta_1$ integrins are found in linear adhesion sites that do not contain AP-2, illustrating that only a fraction of $\alpha_1\beta_1$ integrins are being internalized at any given time. Transmembrane receptors targeted for internalization are recognized by AP-2 through specific sequences in their cytosolic tails. Two of these consensus sequences are YXXø (*43*) and NPXY (*44*, *45*). Introduction of the internalization sequence YXXø is sufficient and necessary for internalization of influenza virus

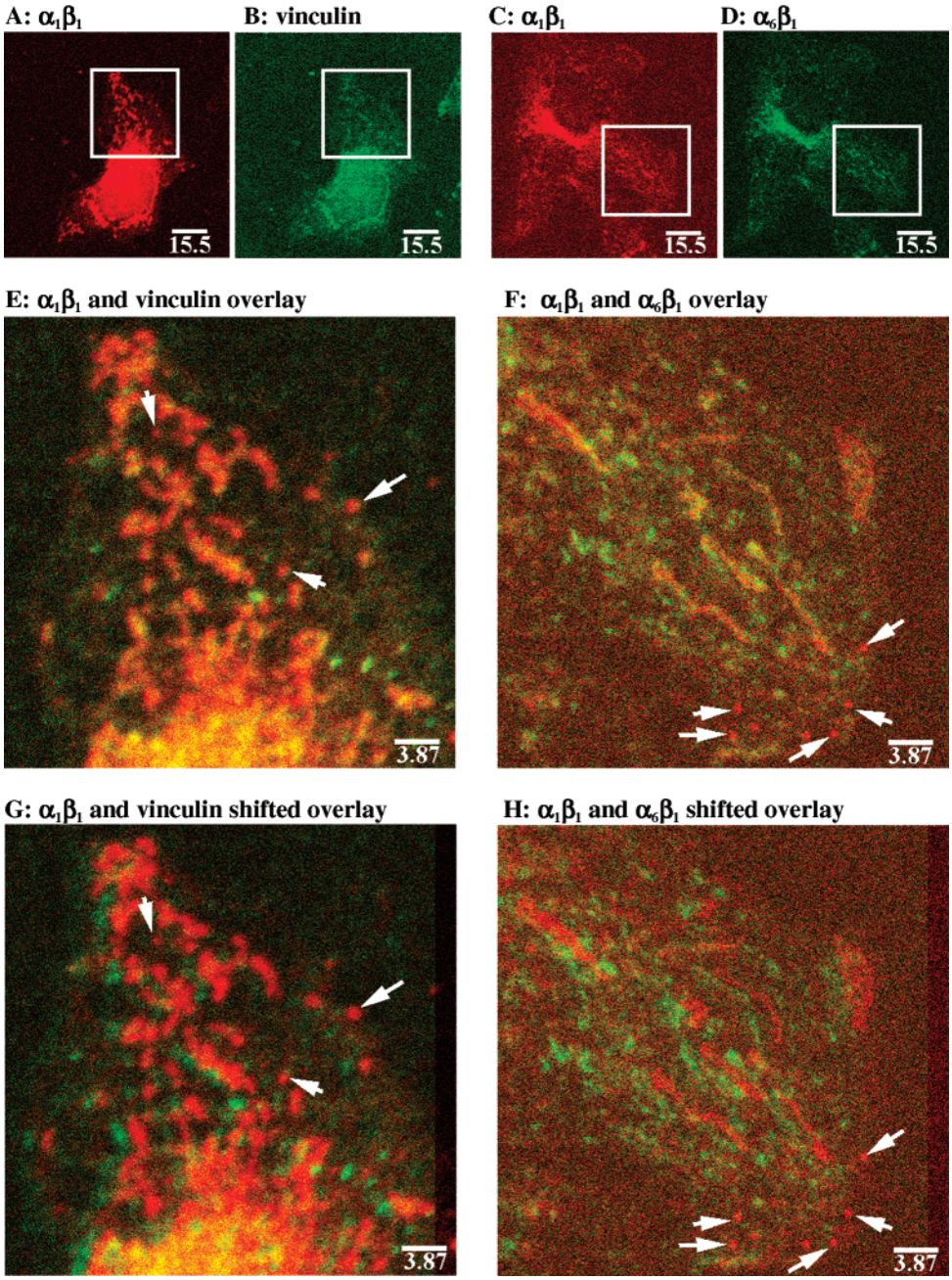

FIGURE 7: Confocal images of RD cells grown on laminin for 24 h were immunolabeled for $\alpha_1\beta_1$ (red) and vinculin (green) or $\alpha_1\beta_1$ (red) and $\alpha_6\beta_1$ (green). Scale bars are shown in micrometers. Low magnification images (scale bar represents 15.5 μm) show the same cell stained for $\alpha_1\beta_1$ (A) and vinculin (B) or $\alpha_1\beta_1$ (C) and $\alpha_6\beta_1$ (D). Higher magnification images (scale bar represents 15.5 μm) from cells shown in (A) and (B) immunolabeled for $\alpha_1\beta_1$ and vinculin, respectively, are shown in (E), and the higher magnification images from cells shown in (C) and (D) immunolabeled for $\alpha_1\beta_1$ and $\alpha_6\beta_1$, respectively, are shown in (F). Regions where the green and red overlap will result in yellow. The green (vinculin or $\alpha_6\beta_1$) images from these overlays (E, F) were shifted 1.8 μm to the left to better visualize individual chromophores. The scale bars are shown in micrometers. Arrows on the overlay images (E−H) indicate areas where there is red chromophore ($\alpha_1\beta_1$) in the absence of green chromophore (vinculin or $\alpha_6\beta_1$), which may correspond to coated pits.

hemagglutinin (*23*). The NPXY motif is conserved in the LDL receptor from six species and is required for endocytosis (*45*). This motif is also found in EGF and insulin receptors which are also internalized through clathrin-coated pits (*39*). It is therefore likely that the β_1 family of integrins may interact with AP-2 through one of the two NPXY sequences located in the β_1 cytosolic tail. Prior to internalization, EGF receptors are found in caveolae where they initiate signaling responses (*58*). Immunoprecipitation experiments have shown that $\alpha_1\beta_1$ and $\alpha_5\beta_1$ integrins, but not $\alpha_2\beta_1$, $\alpha_3\beta_1$, or $\alpha_6\beta_1$ integrins, also associate with caveolin to mediate signaling through the adaptor Shc (*59*). Whether $\alpha_1\beta_1$ integrins located in focal adhesions or caveolae are responsible for signaling AP-2 redistribution is unknown. Evidence from our integrin blocking experiments indicate that signaling from focal adhesions is necessary for the redistribution of AP-2.

The $\alpha_6\beta_1$ integrin also mediates the redistribution of AP-2 to the cell periphery, but unlike $\alpha_1\beta_1$, it does not colocalize with AP-2 in coated pits. Therefore, the internalization and downregulation of $\alpha_6\beta_1$ is likely mediated by mechanisms different from those for $\alpha_1\beta_1$ integrins. If the NPXY motif functions by targeting β_1 integrins to coated pits, it is likely

that this sequence is masked by the α_6 subunit and thus prevents the association of $\alpha_6\beta_1$ with AP-2. However, $\alpha_6\beta_1$ colocalizes with $\alpha_1\beta_1$ integrins in focal adhesions where they generate signals for AP-2 redistribution into the cell periphery, possibly to prepare for endocytosis of $\alpha_1\beta_1$ integrins. We propose that signals generated by receptors associated with caveolae ($\alpha_1\beta_1$ and $\alpha_5\beta_1$ integrins, EGF receptors) are responsible for their subsequent association with AP-2; those receptors that do not associate with caveolin ($\alpha_2\beta_1$, $\alpha_3\beta_1$, and $\alpha_6\beta_1$ integrins) do not move into coated pits. This would predict that $\alpha_5\beta_1$ integrins which also associate with caveolin (*59*) would be internalized while $\alpha_2\beta_1$ and $\alpha_3\beta_1$ integrins which do not associate with caveolin would not associate with coated pits.

ACKNOWLEDGMENT

We thank Dr. Margaret S. Robinson (University of Cambridge, U.K.) for providing the AC1-M11-producing antibodies, Dr. Thomas Kirchhausen (Harvard University, Boston, MA) for the polyclonal AP-2 antibody, and Dr. Sashi Uniyal for providing the FB12, GoH3, and TS2/7 antibodies and for providing and helping to purify the MA6 antibody.

REFERENCES

1. Prasad, K., and Keen, J. H. (1991) *Biochemistry 30*, 5590−5597.
2. Heuser, J. E., and Keen, J. (1988) *J. Cell Biol. 107*, 877−886.
3. Marks, M. S., Ohno, H., Kirchhausen, T., and Bonifacino, J. S. (1997) *Trends Cell Biol. 7*, 124−128.
4. Pearse, B. M., and Robinson, M. S. (1990) *Annu. Rev. Biochem. 6*, 151−171.
5. Schmid, S. L. (1997) *Annu. Rev. Biochem. 66*, 511−548.
6. Ungewickell, E., and Branton, D. (1981) *Nature 289*, 420−422.
7. Kirchhausen, T., and Harrison, S. C. (1981) *Cell 23*, 755−761.
8. Vigers, G. P., Crowther, R. A., and Pearse, B. M. (1986) *EMBO J. 5*, 2079−2085.
9. Shih, W., Gallusser, A., and Kirchhausen, T. (1995) *J. Biol. Chem. 270*, 31083−31090.
10. Gallusser, A., and Kirchhausen, T. (1993) *EMBO J. 12*, 5237−5244.
11. Heuser, J. E., and Anderson, R. G. (1989) *J. Cell Biol. 108*, 389−400.
12. Kirchhausen, T. (1993) *Curr. Opin. Struct. Biol. 3*, 182−188.
13. Robinson, M. S. (1987) *J. Cell Biol. 104*, 887−895.
14. Benmerah, A., Gagnon, J., Begue, B., Megarbane, B., Dautry-Varsat, A., and Cerf-Bensussan, N. (1995) *J. Cell Biol. 131*, 1831−1838.
15. Tebar, F., Sorkina, T., Sorkin, A., Ericsson, M., and Kirchhausen, T. (1996) *J. Biol. Chem. 271*, 28727−28730.
16. Benmerah, A., Cerf-Bensussan, N., and Dautry-Varsat, A. (2000) *J. Biol. Chem. 275*, 3288−3295.
17. Chen, H., Fre, S., Slepnev, V. I., Capua, M. R., Takei, K., Butler, M. H., Di Fiore, P. P., and De Camilli, P. (1998) *Nature 294*, 793−797.
18. Wang, L. H., Sudhof, T. C., and Anderson, R. G. W. (1995) *J. Biol. Chem. 270*, 10079−10083.
19. Slepnev, V. I., Ochoa, G. C., Butler, M. H., Grabs, D., and De Camilli, P. (1998) *Science 281*, 821−824.
20. David, C., McPherson, P. S., Mundigl, O., and De Camilli, P. (1996) *Proc. Natl. Acad. Sci. U.S.A. 93*, 331−335.
21. Brown, C. M., and Petersen, N. O. (1998) *J. Cell Sci. 111* (Part 2), 271−281.
22. Brown, C. M., Roth, M. G., Henis, Y. I., and Petersen, N. O. (1999) *Biochemistry 38*, 15166−15173.
23. Fire, E., Brown, C. M., Roth, M. G., Henis, Y. I., and Petersen, N. O. (1997) *J. Biol. Chem. 272*, 29538−29545.
24. Sorkin, A., and Waters, C. M. (1993) *BioEssays 15*, 375−382.
25. Marsh, M., and McMahon, H. T. (1999) *Science 285*, 215−220.
26. Hirst, J., and Robinson, M. S. (1998) *Biochim. Biophys. Acta 1404*, 173−193.
27. Kirchhausen, T. (2000) *Annu. Rev. Biochem. 69*, 699−727.
28. Juliano, R. L., and Haskill, S. (1993) *J. Cell Biol. 120*, 577−585.
29. Damsky, C. H., and Werb, Z. (1992) *Curr. Opin. Cell Biol. 4*, 772−781.
30. Schoenwaelder, S. M., and Burridge, K. (1999) *Curr. Opin. Cell Biol. 11*, 274−286.
31. Sastry, S. K., and Horwitz, A. F. (1993) *Curr. Opin. Cell Biol. 5*, 819−831.
32. Hynes, R. O. (1992) *Cell 69*, 11−25.
33. Burridge, K., and Chrzanowska-Wodnicka, M. (1996) *Annu. Rev. Cell Dev. Biol. 12*, 463−518.
34. Keen, J. H., Beck, K. A., Kirchhausen, T., and Jarrett, T. (1991) *J. Biol. Chem. 266*, 7950−7956.
35. Lawson, M. A., and Maxfield, F. R. (1995) *Nature 377*, 75−79.
36. Felsenfeld, D. P., Schwartzberg, P. L., Venegas, A., Tse, R., and Sheetz, M. P. (1999) *Nat. Cell Biol. 1*, 200−206.
37. Van Nhieu, G. T., Krukonis, E. S., Reszka, A. A., Horwitz, A. F., and Isberg, R. R. (1996) *J. Biol. Chem. 271*, 7665−7672.
38. Nicol, A., and Nermut, M. V. (1987) *Eur. J. Cell Biol. 43*, 348−357.
39. Trowbridge, I. S. (1991) *Curr. Opin. Cell Biol. 3*, 634−641.
40. Beltzer, J. P., and Spiess, M. (1991) *EMBO J. 10*, 3735−3742.
41. Nesterov, A., Kurten, R. C., and Gill, G. N. (1995) *J. Biol. Chem. 270*, 6320−6327.
42. Ohno, H., Stewart, J., Fournier, M. C., Bosshart, H., Rhee, I., Miyatake, S., Saito, T., Gallusser, A., Kirchhausen, T., and Bonifacino, J. S. (1995) *Science 269*, 1872−1875.
43. Boll, W., Ohno, H., Songyang, Z., Rapoport, I., Cantley, L. C., Bonifacino, J. S., and Kirchhausen, T. (1996) *EMBO J. 15*, 5789−5795.
44. Trowbridge, I. S., Collawn, J. F., and Hopkins, C. R. (1993) *Annu. Rev. Cell Biol. 9*, 129−161.
45. Chen, W. J., Goldstein, J. L., and Brown, M. S. (1990) *J. Biol. Chem. 265*, 3116−3123.
46. Rothman, J. E., and Wieland, F. T. (1996) *Science 272*, 227−234.
47. Giancotti, F. G., and Ruoslahti, E. (1999) *Science 285*, 1028−1032.
48. Hynes, R. O. (1987) *Cell 48*, 549−554.
49. Chan, B. M., Kassner, P. D., Schiro, J. A., Byers, H. R., Kupper, T. S., and Hemler, M. E. (1992) *Cell 68*, 1051−1060.
50. St. Pierre, P. R., and Petersen, N. O. (1992) *Biochemistry 31*, 2459−2463.
51. Petersen, N. O., Höddelius, P. L., Wiseman, P. W., Seger, O., and Magnusson, K. E. (1993) *Biophys. J. 65*, 1135−1146.
52. Wiseman, P. W., Höddelius, P., Petersen, N. O., and Magnusson, K. E. (1997) *FEBS Lett. 401*, 43−48.
53. Brown, C. M., and Petersen, N. O. (1999) *Biochem. Cell Biol. 77*, 439−448.
54. Petersen, N. O. (2001) in *Fluorescence Correlation Spectroscopy Theory and Applications* (Rigler, R., and Elson, E. S., Eds.) pp 162−184, Springer, Berlin.
55. Wiseman, P. W., and Petersen, N. O. (1999) *Biophys. J. 76*, 963−977.
56. Robinson, M. S. (1994) *Curr. Opin. Cell Biol. 6*, 538−544.
57. Smythe, E., and Warren, G. (1991) *Eur. J. Biochem. 202*, 689−699.
58. Mineo, C., Gill, G. N., and Anderson, R. G. (1999) *J. Biol. Chem. 274*, 30636−30643.
59. Wary, K. K., Mainiero, F., Isakoff, S. J., Marcantonio, E. E., and Giancotti, F. G. (1996) *Cell 87*, 733−743.

BI011501F